

## High Fidelity Aerodynamics Models for Blended Wing Body Design

Luca CERQUETANI<sup>1\*</sup>, Alessandro SGUEGLIA<sup>1</sup>, Emmanuel BENARD<sup>1</sup>, Peter SCHMOLLGRUBER<sup>2</sup>

<sup>1</sup>ISAE-SUPAERO, 10 av. Edouard Belin, 31055 Toulouse, France

<sup>2</sup>ONERA, 2 av. Edouard Belin, 31055 Toulouse, France

\*Corresponding author: Luca CERQUETANI, ISAE-SUPAERO, 10 av. Edouard Belin, 31055 Toulouse, France. Tel: +393341471518; Email: lucacerquetani95@gmail.com

**Citation:** CERQUETANI L, SGUEGLIA A, BENARD E, SCHMOLLGRUBER P (2018) High Fidelity Aerodynamics Models for Blended Wing Body Design. Int Jr Rob and Auto Engg: IJARE-103.

**Received Date:** 17<sup>th</sup> August, 2018; **Accepted Date:** 22<sup>nd</sup> August, 2018; **Published Date:** 3<sup>rd</sup> September, 2018

### Abstract:

*The Blended Wing Body (BWB) configuration is seen by many as one of the possible future protagonists of Civil Aviation, both for its potential benefits in terms of Aerodynamics performances and fuel consumption and for the possibility of incorporating Aero-Propulsive integration technology. However, the design of such an innovative aircraft does not come without any difficulties, which are mainly related to its unconventional shape and the lack of knowledge. In the framework of the development of a preliminary design tool (FAST), this work aimed at creating a High Fidelity Aerodynamics Model of the ISAE-OENRA BWB geometry, whose main purpose was the validation of the Lower Fidelity tools which are implemented at early stage phases of BWB design. The development of such a method allowed also to verify important properties of the flow around the geometry like efficiency, compressibility and trim, and paved the way to a further study of the stability and the control of the BWB configuration. The limits of this approach are to be found in the characteristics of the method (Euler equations) and its incapacity to picture important effects like friction Drag and separation. The following step of the research will be the implementation of a RANS model of the geometry.*

### 1. Introduction

Performances improvement and fuel consumption reduction are just two of the many challenges which characterize the future of civil aviation and boost the work of researchers and engineers. The classical "wing-tube" configuration for civil transport aircraft has been thoroughly developed in the last 60 years, leading to constant progress in all the disciplines involved in Aeronautics (from design phase to operational life, from manufacturing to maintenance). Nevertheless, the common perception nowadays is that the key to reach higher standards in fuel

consumption and Aerodynamics performances is to develop and propose practical solutions for non-conventional aircraft designs, such as the Blended Wing Body (BWB) [1-4]. The great advantage brought by this configuration consists in higher values for L/D ratio, mostly due to its lower wetted area to volume ratio and lower interference drag, with a clear gain in fuel consumption. However, many challenges arise: difficult parametric shape design, pressurization, trim and stability [3].

Many studies have been carried out in the last 20 years to characterize the aerodynamics properties of

classical BWB geometry, draw conclusions on the choice of some standard design parameters and propose optimization strategies. The majority of these papers highlights the importance of reliability and cost efficiency in aerodynamics computations to fasten optimization routines and get accurate and consistent results. However, so far no systematic study capable of merging Drag and consumption minimization, trim and stability constraints, structure constraints and propulsion integration has been carried out [3].

FAST [5] is a software that has been developed by ONERA and ISAE-SUPAERO to perform preliminary design and optimization of the classical "wing-tube" configuration aircraft, and which is now being updated to be applied on Blended Wing Body unconventional configuration. The research behind the development of such a powerful tool needs the collaboration and the involvement of many disciplines, whose contribution may take different forms: results validation, models comparison and analysis, methodology study and information collection. In this context, the purpose of this work was to develop a High Fidelity Aerodynamics model of the Blended Wing Body geometry to test the methodology, collect information, verify Aerodynamics and Gas Dynamics properties and compare with results obtained with other methods. In particular, the philosophical approach which constitutes the basis of this work consists in validating Low Fidelity preliminary design methods (FAST, VLM) using a High Fidelity model. The project therefore aims at running Computational Fluid Dynamics (CFD) simulations, structured on one of the main sets of equations derived from Navier-Stokes equations and which constitute the basis of the numerical methods in Aerodynamics: Euler equations. The method has been fully developed and simulation cases have been studied. Compressibility, stability and efficiency are just some of the topics that have been studied thanks to the results of these simulations.

This paper contains a description of all the steps which contributed to shape the methodology: familiarization with ISAE-ONERA Blended Wing Body geometry, creation of the mesh, choice of the solver and of the setting of the simulation parameters, data collection and results analysis.

## 2. Geometry

This section contains a description of the geometry considered during this work. The ISAE-ONERA BWB geometry is designed for short range

commercial flight (among the considered TLARs there are 2750 NM range and 150 PAX) and cruise Mach number equal to 0.78. The total surface is 313 m<sup>2</sup>, the mean aerodynamic chord (MAC) is 10.79 m long, and the wingspan is equal to 41 m. The MTOW is approximately 90 tons. The geometry is characterized by two distinct sections. The central body features reflex camber profiles (MH 78\_0\_V2), which allow to get longitudinal stability for the BWB "flying wing" configuration, which indeed does not include an horizontal tail-plane (HTP) [1]. This part of the aircraft should host the passengers and most of the aircraft systems during commercial flight and it is thus pressurized. Above the upper surface of the central body two pylons are mounted, which sustain the two high-bypass ratio turbofan engines and their nacelles. Even though the BWB concept classically allows to implement Aero-Propulsive integration solutions, the choice was made to study independently BWB preliminary design (via FAST) and unconventional propulsion configurations, and then eventually merge the results of the two studies as a further step of the analysis. The root chord (in the symmetry plane) measures 20 m. The center of gravity (CG) of the A/C is located on the symmetry plane at a distance equal to approximately one third of the root chord from the nose of the aircraft. The outer wing features supercritical profiles (NASA SC(2)-0410), which reduce shocks strength and thus wave drag, delaying the phenomenon of drag divergence. Compressibility effects are mainly located in this part of the aircraft surface during design cruise flight, which results in a clear benefit in terms of passenger comfort [1]. The sweep angle of the outer wing is 30° (Figure 1).

The purpose of the work was to study the Aerodynamics properties of the aircraft in clean configuration (nacelles, engines and pylons are therefore not included), so they were removed to create the Aerodynamics model. Finally, it is important to mention that the geometry considered in this work is not optimized yet.

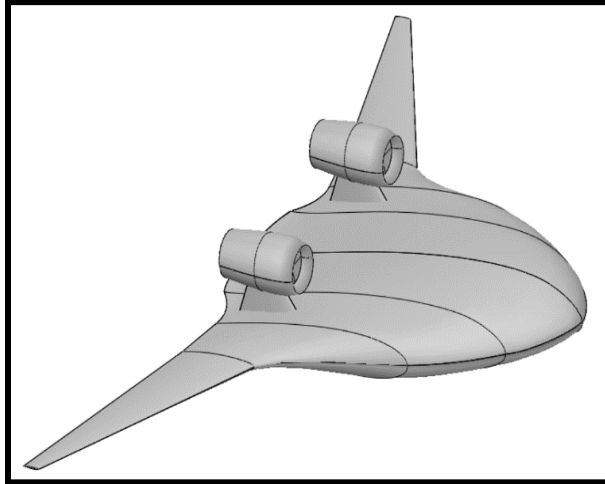


**Figure 1:** The BWB geometry studied in this work.

### 3. Methodology

The goal of the work was creating a High Fidelity Aerodynamics model of the BWB to support the developing of a preliminary design tool. The choice of the method has fallen upon Euler equations, solved by the open source CFD software SU2 [6], which implements a Finite Volume Method. SU2 is a collection of codes which can perform either viscous or in viscid simulations, as well as optimization routines. Validation of SU2 has been the subject of a Master Thesis at ISAE-SUPAERO [7]. Creating a mesh of the geometry is the first step of the development of a CFD model. The designated software to create the mesh was ICEM CFD, the meshing tool of ANSYS [8].

This section contains a description of the characteristics of the methodology, which includes both the creation of the mesh and the definition of the numerical method.

#### 3.1. Mesh Characteristics

A mesh is the partition of the space surrounding the body, occupied by fluid, in many "control volumes", defined by nodes. It is a fundamental step when developing a numerical method like Finite Volume Method (FVM), and the quality of the approximated flow solution depends highly on the level of refinement of the mesh. The mesh that was created for the purpose of this work is structured.

After importing the Blended Wing Body geometry in the meshing tool, the 3D solid space

around the body, which represents the fluid, was created. Since the problem is symmetric, only half of the BWB surface is meshed. The body was placed at the center of a prismatic volume, whose external surface was divided in 6 different regions: Upper and Bottom surfaces, Inlet, Outlet, Lateral surfaces and Symmetry plane. The Inlet surface (which has a curved "C" shape) represents the origin of the incoming flow (upstream flow), while the Outlet surface (a rectangle) closes the region behind the body, where the wake is to be found. These two surfaces are located at a distance of 10 Medium Aerodynamics Chords from the BWB. The Symmetry plane cuts in half the BWB. The Lateral field, Upper and Bottom surfaces close the solid volume ensuring mass conservation. These last surfaces are located at a distance of 6 to 8 medium aerodynamics chords from the BWB (**Figure 2**).

Once the solid volume has been created, it must be divided in several regions surrounding the body. This is due to the fact that the cells size and concentration will vary in the different regions around the body, and this spatial division will enable to account for these differences. The blocks take into account the geometric shape of the Blended Wing Body.

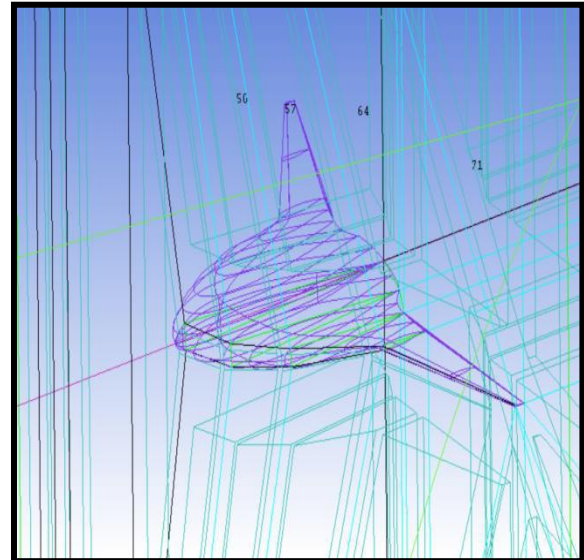


**Fig 2:** Blocks division of the fluid space around the BWB surface.

The fluid blocks reflect this division of the aircraft surface, and are structured, through proper association with the aircraft profiles, in order to follow the curvature of the upper and lower surfaces of the BWB. We could identify a total of 26 blocks.

Last part of the work was then defining the cells size and concentration for each block. In other words, positioning the nodes and establishing location and dimension of the "control volumes". The criteria for doing this are the following:

- More cells are required in the fluid space in proximity of the body than in the far field flow.
- Leading edges, trailing edges, curvature changing regions, airfoils' upper surface (especially for supercritical profiles) and the aircraft wake are the most important regions where the mesh had to be carefully refined.
- Transition between cells dimension must be gradual and sharp changes in cells size must be in general avoided (except for far field).
- Non-orthogonality between cells must in general be avoided.
- The total number of cells must be big enough for the mesh to be satisfactorily accurate, but not too big (especially if unnecessary) to allow fast convergence.

The mesh features a total of 8 million cells, 11 thousands of which are in contact with the BWB surface, which is roughly divided in 80 partitions in the span-wise direction and 70 in the chord-wise direction (**Figure 3**).

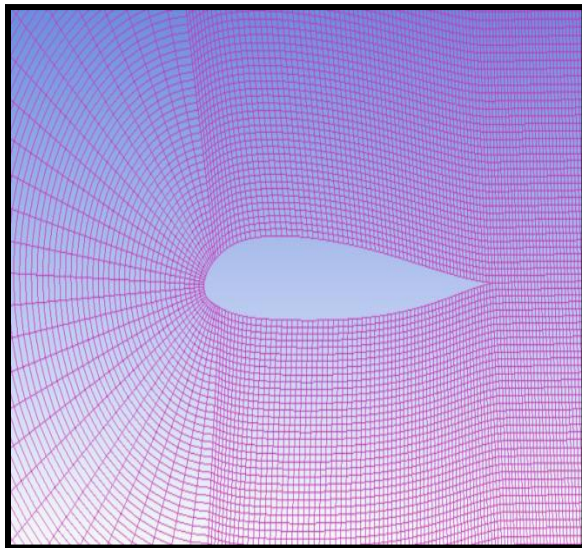


**Figure 3:** Detail of mesh around the BWB surface (symmetry plane).

### 3.2. Numerical Method

This section contains an overview of the settings of the numerical method which was implemented in this work. The parameters of the simulations are contained in a configuration file, which is one of the two input files (the other one is the mesh of the geometry) required by SU2 to launch the computations.

First of all, it is required to define the kind of method SU2 will have to implement to solve the problem, which in our case are Euler equations in compressible flow. Then, the properties of the upstream flow are defined. Some of them did not change between one simulation and another. This is the case of the Static Pressure and the Temperature. It is also required to specify the fluid model (Standard Air) and some of its properties (like the specific heats ratio and the specific Gas constant). On the contrary, some other properties would change according to the kind of simulations we wanted to perform and the results we want to obtain. These quantities are the Mach number ( $M_\infty$ ), the angle of attack ( $\alpha$ ). The next step was the definition of the reference quantities, which come from the geometric characteristics of the geometry (MAC and reference surface) and which will be used by the software to make Lift, Drag and the Aerodynamic Momentum non dimensional. It was also required to specify the point with respect to which the Momentum is computed (25% of MAC).

A crucial point was the choice of the boundary conditions to assign to the external surfaces of the fluid solid volume and to the BWB surface. "Slip" boundary conditions (called "Euler wall" conditions by SU2) have been assigned to the BWB surface and to the Lateral surface. "Far field" boundary conditions have been assigned to the Inlet, to the Outlet and to the Upper and Bottom surfaces. Finally, "Symmetry" boundary conditions have been assigned to the Symmetry plane. The choice of "Slip" conditions for the BWB surface come from the fact that viscosity is not included in Euler equations model (**Figure 4**).

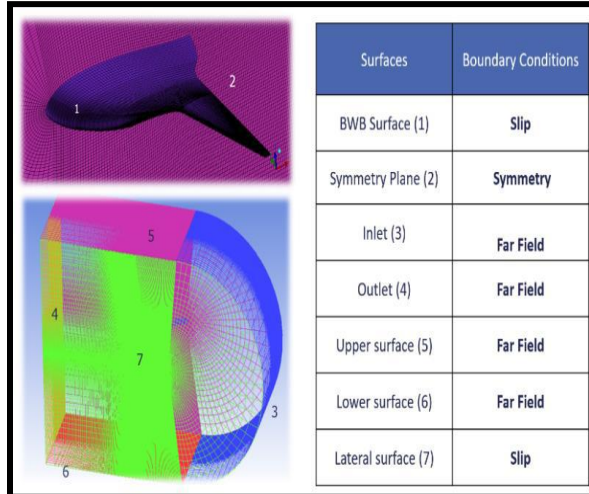


Figure 4: Summary of Boundary conditions.

It was then important to carefully define the settings for the numerical method of the solver. The choices for these parameters have been made mainly on a trial and error basis, studying the convergence of the solution and the time and number of iterations required, even though a preliminary knowledge of the characteristics of each method was used to make an initial selection of models. The reference that constituted the basis of this approach was Computational methods for Fluid Dynamics by Ferziger-Péric [9]. The convergence of the solution was based on the history of the  $CL$ ,  $CD$  and  $CM$  coefficients, analyzing their evolution at each iteration.

In fact, the numerical method for spatial gradients, the linear solver and the convective numerical method highly depend on the mesh which is being used. So, it is not possible to establish with certitude the efficiency of a certain set of parameters without really launching simulations and having a look to the results. This is the reason why several trials have been made before fixing the parameters which would then be used throughout the entire simulation cycles. The main settings are reported hereafter:

- The choice of the convective numerical method fell upon Jameson-Schmidt-Turkel (JST) scheme, even though Lax-Friedrich and Roe methods were also considered and tested. The reason for this choice was that JST method always allowed to reach convergence (both in subsonic and transonic regimes), and it managed to describe efficiently pressure and local Mach number profiles around the BWB surface.

- The choice for the iterative solver of the linear system was made between Flexible Generalized Minimal Residual methods (FGMRES), Jacobi method and incomplete LU (ILU) factorization. The choice was made on a trial and error basis, and it finally fell upon ILU scheme, since it was the one that allowed to get faster convergence, in terms of both time required and number of iterations.
- The numerical method for spatial gradients which was adopted in this work is the Green Gauss method, which was the default setting of the configuration file. A related parameter which is dramatically important for the simulation convergence (especially in terms of time required and number of iterations) is the Courant–Friedrichs–Lewy (CFL) condition. The bigger is this parameter, the faster convergence is reached. These results were observed and confirmed in all the tests made before the beginning of the real simulations. However, the value of the CFL coefficient should not exceed 1, since in some cases this could result in the divergence of the iterative procedure, condition which was obtained in some of the tests performed. The value of the CFL coefficient was finally set to 0.95, an intermediate value which allowed to get relatively fast results without triggering the divergence of the flow solution.
- Finally, Van Albada function was chosen for the slope limiter (flux limiter) (Table 1).

Numerical Method Parameters	
Convective Numerical Method	Jameson-Schmidt-Turkel (JST)
Iterative Solver of Linear System	Incomplete LU (ILU) factorization
Numerical Method for spatial gradients	Green Gauss method
CFL coefficient	0.95
Slope limiter(flux limiter)	Van Albada function

Table 1: Main settings of the numerical method.

Now that we have presented in details the characteristics of the mesh and of the configuration file, we shall proceed with the presentation and the analysis of the results obtained with the simulations.

#### 4. Results

This section contains the results obtain with the cycles of simulations. Before presenting them, we will first have an overview of the simulation cases which were analyzed:

- A first series of simulations was performed at high speed, meaning that the Mach number ( $M_\infty$ ) was set to 0.78 (design cruise condition) and the angle of attack would change at each simulation, ranging from  $-2^\circ$  to  $7^\circ$ . Compressibility, stability and efficiency are only some of the topics that were analyzed with the results of these computations.
- The second series of simulations was performed at low speed, meaning that the Mach number in the configuration file was this time set to 0.3. As in the previous case, the angle of attack would range from  $-2^\circ$  to  $7^\circ$ .
- The third and last series of simulations was performed with a completely different approach, allowing to study the evolution of the Drag produced by the BWB geometry as a function of the Mach number, that is to say considering the effects of compressibility (supersonic pockets, shocks and wave drag) on the total Drag of the aircraft. The angle of attack of the upstream flow was therefore fixed and set to  $1.5^\circ$ , and the upstream Mach number would now change at each simulation, ranging from 0.3 to 0.9 (from subsonic to fully transonic regime).

The total number of simulations was 21. Each one took approximately 24 hours, even if the converging time would strongly depend on the angle of attack and on the Mach number. In the next paragraphs the most important results obtained for each cycles of simulations will be commented.

##### 4.1. High Speed

The most important application of high speed results is the comparison with computations performed with Lower Fidelity tools. These tools are Open VSP [10], which implements a Vortex Lattice Method and adopts Karman-Tsien correction to account for compressibility, and FAST [5], which computes the Aerodynamic Polar using analytic and semi-empirical formulas included in AIRBUS/SUPAERO handbook from preliminary design [11] (Table 2).

Method	$C_{L_\alpha} [ \frac{1}{rad} ]$
FAST	4.6
OpenVSP (VLM)	4.9
SU2(CFD- Euler)	4.5

**Table 2:** Comparison of  $CL_\alpha$  coefficients.

As it is shown in Figure 6, the  $CL_\alpha$  coefficients computed with the three different methods are rather consistent (the discrepancies are smaller than 10%). If we have a look to the  $CL - \alpha$  plot comparison (Figure 5), we see that while SU2 and OpenVSP tend to give similar results in the range  $2^\circ - 5^\circ$ , OpenVSP tends to overestimate the  $CL$  coefficient for  $\alpha > 7^\circ$ . Besides,  $CL_0$  is higher for CFD.

The reasons of these differences are to be found in the different approaches on which the two methods are built.

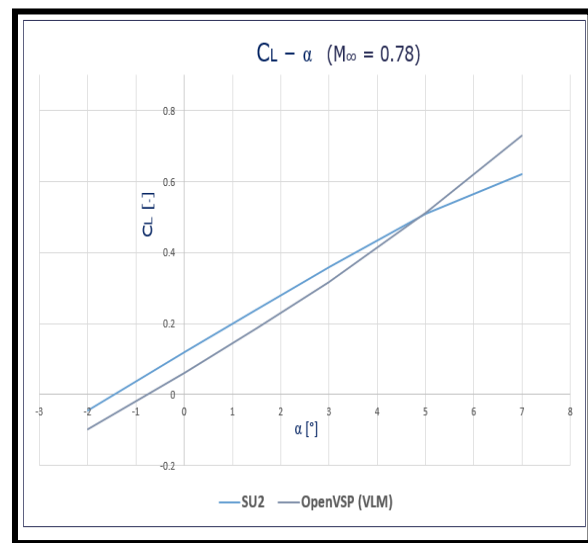


**Figure 5:** Comparison of  $CL - \alpha$  plots ( $M_\infty=0.78$ ).

VLM models are based on potential flow and on an extension of Prandtl Lifting-line theories; they do not consider the thickness of the body and mainly compute an incompressible solution, which is then adjusted with a corrective term only at a second stage. Euler equations on the contrary allow direct computation of compressibility effects and take into account geometric characteristics like the thickness of the lifting surface. It is therefore expected that Open VSP would overestimate the Lift coefficient for high angles of attack. Nevertheless, we can conclude that around cruise angle of attack (estimated between  $2.5^\circ$  and  $3.5^\circ$ ) the 3D Lift properties are described

with acceptable degree of accuracy by the Lower Fidelity tool. This is a useful result to analyze the comparison of the Polar curves (**Figure 6**), which includes also the Polar computed with FAST. Neglecting region 2 of the graph (which corresponds to not feasible cruise flight points), one can see in region 1 that FAST and Open VSP rather underestimate the  $C_D$  coefficient for a given  $C_L$ . Since the induced Drag computed by the three models is homogeneous (as a consequence of 3D Lift properties being pictured in consistent way, as we demonstrated comparing  $CLa$  coefficients and  $CL-\alpha$  plots), the difference in the values of the  $C_D$  is due to the computation of Wave Drag.

In fact, while on one hand with Euler equations we have direct computations of compressibility effects (and thus proper representation of supersonic pockets and shocks), on the other side we have Karman-Tsien correction for Open VSP and semi-empirical graphs for FAST, which inevitably lead to an underestimation of Wave Drag, especially for high angles of attack. Once again, neglecting the thickness is also a crucial aspect that must be taken into account while validating these results.

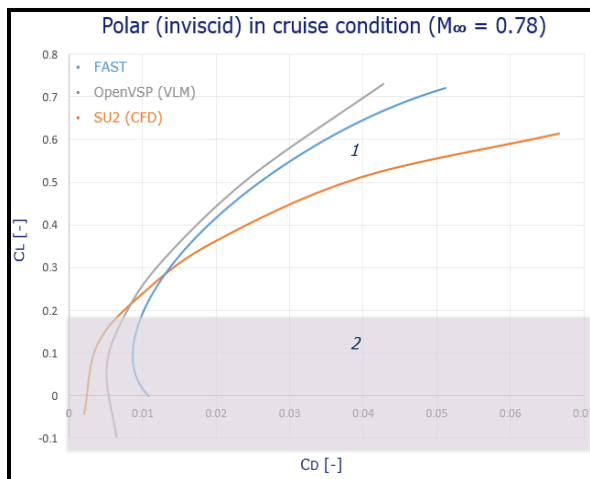


**Figure 6:** Comparison of Polar curves ( $M_\infty=0.78$ ).

The comparison of FAST and SU2 Aerodynamics Polar must be considered in the framework of the research upon BWB preliminary design and optimization. Comparing the two flow solutions in terms of Lift and Drag coefficients highlighted the need of corrective terms to implement in FAST to adjust the results, taking into account the results of CFD model (which intervenes here as a validating tool). In fact, and this can indeed be considered true for Open VSP too, lower fidelity methods require less computational time, and are in general more suitable

for preliminary design studies and optimization routines. Higher fidelity methods are then used at a second stage to validate the results of lower fidelity tools, to check the consistency of the computations.

The reason why the SU2 polar was not directly implemented into FAST, is that the latter is an optimization software, which needs to perform the same Aerodynamics computations at each iteration. Thus, it was considered better to keep the FAST analytic model in the tool, adding the corrective terms to take into account high fidelity validation. The corrective terms have been derived for just one flight condition (cruise Mach number), by comparison of the Polar curves. This preliminary approach can be extended with further comparisons at other flight points, and a regression law could be derived to link the results in a more efficient way, allowing increasing the accuracy of the computations in FAST.

Another important topic of Blended Wing Body Aerodynamics analysis is efficiency. Better performances in terms of Lift to drag ratio are one of the reasons why the Flying Wing unconventional configuration has been studied in the past 20 years and could be one of the possible future steps of commercial aviation [1]. The absence of abrupt transition between wing and fuselage leads to smaller interference drag (parasite drag), and there is an overall decrease on the wetted area to volume ratio. These two effects lead to an increase in the Lift to drag ratio, with clear gains in terms of fuel consumption.

(**Figure 7**) shows the Lift to drag ratio as a function of the  $C_L$  coefficient. The picture contains two different plots. The orange curve shows the results coming directly from high speed simulations with SU2. This flow solution does not account for viscosity, which is indeed not pictured by Euler equations. A possible answer to the problem, which leads to a mixture of low and high fidelity methods, is adding to CFD results a corrective term to include skin friction. For the purpose of this work, we considered a constant  $C_{D0}$  term computed in Open VSP using Moody Charts and we added it to SU2 computations. The result is represented in (**Figure 9**) by the blue curve, which is indeed lower than the orange one. The computations gave a first estimate of the Maximum Lift to drag ratio of ISAE-ONERA BWB geometry of approximately 23 (reached for an angle of attack between  $2^\circ$  and  $3^\circ$ ) which is indeed higher than the traditional values for "wing-tube" airliners (15-17). It is also important to remark that the current BWB geometry is not optimized.

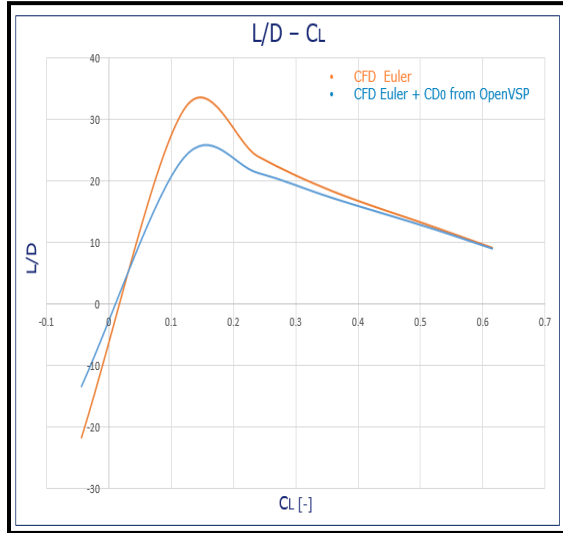


Figure 7: Efficiency curves for BWB at  $M_{\infty}=0.78$ .

#### 4.2. Low Speed

Results at low speed ( $M_{\infty} = 0.3$ ) have been used to validate Low Fidelity tools (like FAST) in similar way to what has been show in the previous paragraph for high speed. Another crucial aspect of Blended Wing Body design is longitudinal stability, since Flying Wings do not include a horizontal tail-plane (HTP) to participate in the aircraft's balancing. In order for an aircraft whit such geometric characteristics to be stable, the following conditions must be true: the center of gravity must be forward with respect to the Aerodynamic Center (located with good approximation at 25% of Mean Aerodynamic Chord), and the Aerodynamic Moment computed at the Aerodynamic Center (also called neutral point) must be pitch-up (negative in the usual convention) [12, 13].

From preliminary design data (first non-optimized design) the center of gravity (CG) is located at 30% of the root chord (symmetry plane of BWB), which corresponds to a distance of 6.67 meters from the nose point, while 25% of MAC is located at 9.15 meters from the nose point. The way to have pitch-up aerodynamic moment in a Flying Wing configuration is using reflex camber profiles. ISAE-ONERA BWB configuration features reflex camber profiles (MH 78\_0\_V2) in the central body.

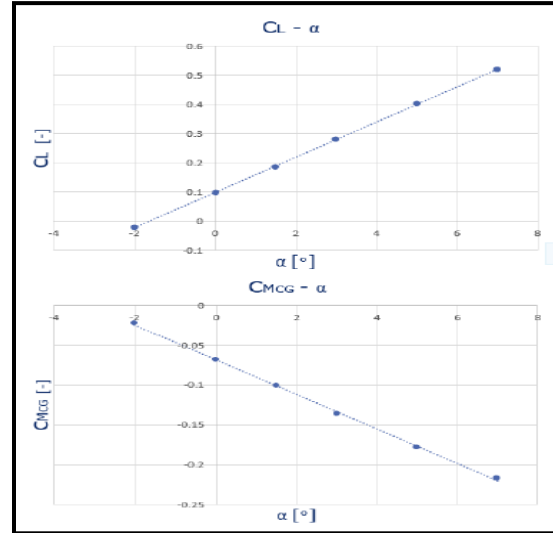


Figure 8:  $CL-\alpha$  and  $CM-\alpha$  curves for BWB at low speed ( $M_{\infty}=0.3$ ).

BWB stability has been studied in this work at low speed since compressibility effects tend to move the Aerodynamic center backwards (thus increasing stability), so proving that the aircraft is stable at subsonic regime automatically implies that the aircraft is stable at cruise flight. Useful criteria to prove the stability of an aircraft is the static margin:

$$S.M = \frac{C_{M_{CG}}}{C_{L_{\alpha}}}$$

The static margin is a direct measure of longitudinal static stability. For static stability, the static margin must be positive. Moreover, the larger the static margin, the more stable is the aircraft [13].

From graphs (Figure 8), we get that the  $CMCG$  coefficient with respect to the center of gravity is equal to -2.04 and the  $CL\alpha$  coefficient is equal to 3.46. We finally get:

$$S.M = \frac{C_{M_{CG}}}{C_{L_{\alpha}}} = 0.59$$

This result validates computations performed with FAST, which gave a value of the static margin of 0.54. This proves that the aircraft is stable, even though the stability margin is surprisingly big (almost 60%). However, it is necessary to recall that the geometry is not optimized.

### 4.3. Mach Sensitivity study

The last series of simulations has been performed with the logic of studying the evolution of the total Drag produced by the BWB as a function of the Mach number, that is to say as a result of compressibility effects such as supersonic pockets and shock waves. Instead of fixing the upstream Mach number as we did for the previous two cases, in this cycle we set the angle of attack to a fixed value ( $1.5^\circ$ ) and we performed different simulations for increasing values of the upstream Mach number, from 0.3 to 0.9. Results are shown in (Figure 9).

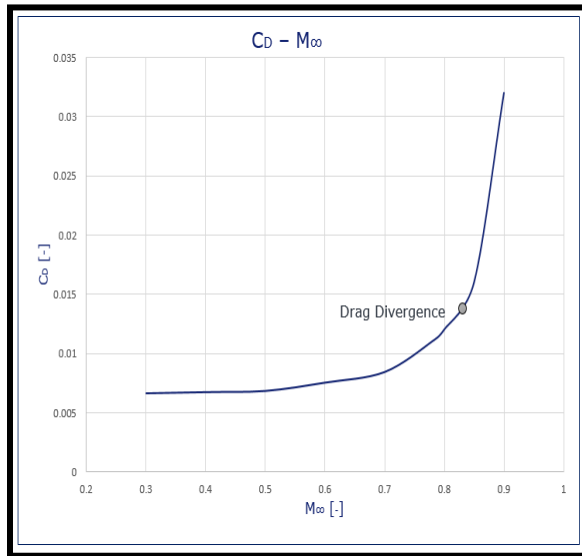


Figure 9:  $C_D - M_\infty$  curve for BWB.

One can immediately notice that the Drag stays almost constant up to the transonic regime, which starts between Mach 0.7 and 0.8. In subsonic regime, the only Drag component pictured by SU2 simulations is induced Drag, since no parasite Drag or friction Drag are involved in Euler equations method. Moreover, since viscosity is not considered, unexpected pressure recoveries at the trailing edge lead to a null value of pressure Drag (D'Alembert paradox). When the upstream Mach number reaches the critical Mach number value (which is smaller than 1) supersonic pockets start to form on the BWB upper surface as a result of flow expansion downstream the leading edge (mainly in the outer wing) and shocks occur. The dimension of the supersonic pockets and the strength of the shocks increase with the upstream Mach number. This leads to an increase of the total Drag, due to the contribution of wave Drag. Once the transonic regime is entered, Drag starts to increase sharply [12]. The point which is usually considered as the

beginning of the Drag Divergence corresponds to the point of the  $C_D - M_\infty$  curve where the derivative is equal to 0.1 (10 %). From the results of SU2 simulation, for ISAE-ONERA Blended Wing Body geometry, this point corresponds to a Mach number of 0.83 (Figure 9) and a total Drag coefficient of 0.0014, more than twice the value at low speed. This means that wave drag already accounts for more than 50% of the total drag produced by the A/C. One can notice that the Drag Divergence pattern of the BWB is consistent with the one of supercritical profiles (in particular the phenomenon Drag divergence occurring at Mach 0.82-0.83). In fact, especially at early transonic regime, compressibility effects are mainly located in the outer wing, where supercritical profiles are located. This means that the shocks that are occurring are relatively weak, wave Drag is contained and Drag divergence is delayed.

We will now end this paragraph, and the section of this report dedicated to results, by showing a 3D visualization of the Mach flow around the whole BWB surface, for three different values of the upstream Mach number. These pictures will allow us to go through some of the phenomena we have analyzed so far. (Figure 10) shows the local Mach flow at  $M_\infty = 0.80$ . One can clearly see that compressibility effects are mainly located in the outer wing, where shocks can be seen. On the contrary, in the central body, supersonic pockets are much smaller compared to chords length, and the local Mach number goes slightly above 1. Compressibility effects are still weak. This condition is the best possible for passengers comfort (and efficiency / fuel consumption), even though we already are slightly above design cruise Mach. In (Figure 11), the upstream Mach number is now 0.85. Since compressibility is a very sharp phenomenon, especially at transonic regime, small changes in the Mach number can lead to big effects on the flow around the body [14, 15].

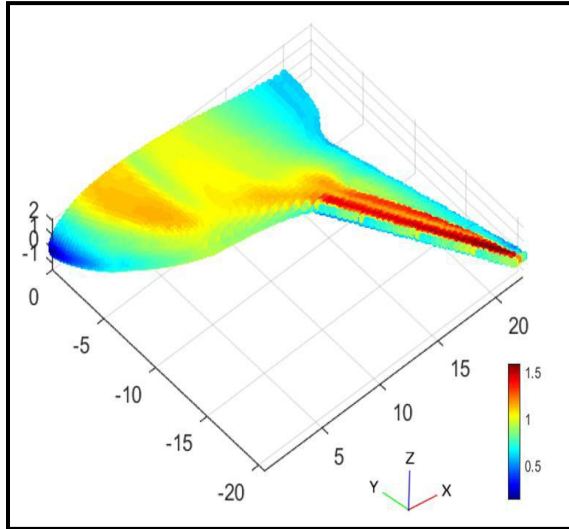


Figure 10: Local Mach flow for  $M_\infty = 0.8$ .

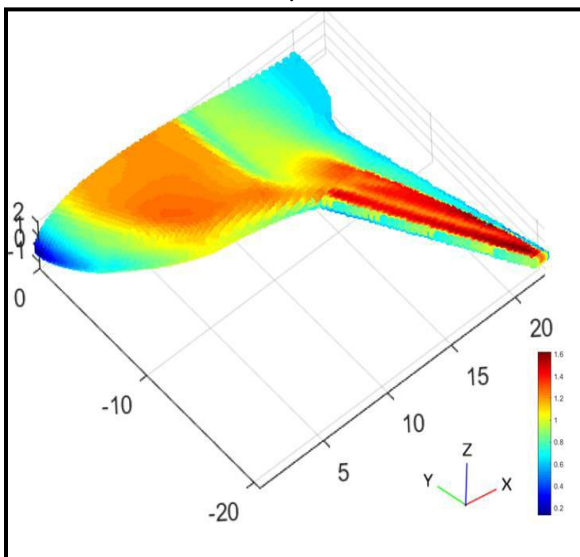


Figure 11: Local Mach flow for  $M_\infty = 0.85$ .

Here we can see that now a big shock is occurring even in the central body, and that locally the Mach number has overcome the typical design limits (1.4 / 1.5), which are set to avoid violent and abrupt phenomena of separation and turbulence caused by the strong shock waves. Looking at the Mach profiles in the center body and in the outer wing one may find consistency with classical reference cases for transonic flow around airfoils [12]. The center body features reflex camber profiles, which are not designed explicitly for transonic regime. The shock occurs at half the upper surface, and it is indeed quite strong. The supersonic pocket which is found on the

outer wing is on the contrary relatively wide compared to the chord length, and an isentropic compression precedes the shock, which is thus weaker. This case study is way above design cruise Mach and the total Drag has already diverged, leading to a dramatic loss of efficiency.

If we increase again the free field Mach number (now equal to 0.90) we can see that compressibility effects, which were located initially only in the upper surface, now start to be present also in the lower surface (Figure 12). If we increase again the upstream Mach number (approaching 1, full supersonic flight condition) we will see that the shocks will get closer and closer to the trailing edge, and that a big detached shock will also form in front of the leading edge [12].

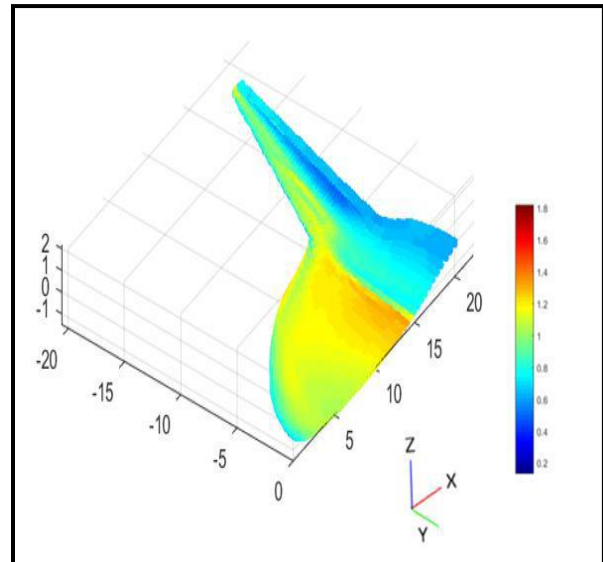


Figure 12: Local Mach flow for  $M_\infty = 0.9$ .

## 5. Conclusions and Perspectives

This paper has shown how, starting from the Blended Wing Body ISAE-ONERA geometry only, it has been possible to run Computational Fluid Dynamics (CFD) simulations to obtain common Aerodynamics results and verify classical macroscopic flow properties[16-21].

One of the many purposes of the development of this model was contributing to Blended Wing Body preliminary design and optimization, by validating lower fidelity methods which are implemented in FAST software (ISAE-ONERA) using a high fidelity tool. This approach allowed also to share useful results and information and to confirm important

assumptions made at the very first stage of design (before optimization itself) concerning compressibility effects, efficiency and stability. This contribution boosted the development of the Aerodynamic tools implemented in FAST, improving the accuracy of the computations and increasing the level of confidence in the results, in terms of Aerodynamics properties and performances of the geometry.

A future application of the results of these simulations will be the study of longitudinal stability and control of BWB geometry, which will allow a better understanding of what is known to be a crucial aspect of Flying Wing configuration. It will be also an opportunity to propose preliminary solutions for control surfaces positioning and control routines implementation.

The limit of the method developed in this work is to be found in the definition itself of the problem, which is structured on the approximated solution of Euler equations. This model does not include viscosity, and thus many important phenomena of the flow around the BWB could not be portrayed with the results of the CFD simulations. Among these phenomena there are skin friction, separation, turbulence and stall, which have important consequences in the Drag computation (friction, parasite and pressure Drag). In this work Friction Drag was included in the model through a corrective term coming from lower fidelity (analytic model). This approach will be improved performing RANS simulations, where the aforementioned flow aspects will be directly computed by the numerical solver. RANS simulations will allow to perform a Drag Breakdown study, improving the understanding of the differences between Low and High Fidelity methods in terms of Drag computation. The acquisition of the methodology has been a key aspect of the work so far, since the same skills (especially in terms of mesh creation and numerical method settings) will be of primary importance while moving on with the next step of the research, which concerns Reynolds-averaged Navier-Stokes equations.

## 6. Acknowledgments

- I gratefully thank Professor Emmanuel Bénard and supervisor Alessandro Sgueglia for the precious guidance and the constant support they have given me throughout this work.
- I also thank AIRBUS © for the support given to the research on Blended Wing Body design through the funding of the CEDAR Chair, which

finances the research of many PhD students at ISAE-SUPAERO and ONERA.

- I finally thank my family for the opportunities they give me every single day through their love and sacrifice.

## References

1. Liebeck RH (2004) Design of the blended wing body subsonic transport. *Journal of aircraft* 41: 10-25.
2. Qin N, Qin A, Vavalle A Le, Moigne M, Laban K, et al. (2004) Aerodynamic considerations of blended wing body aircraft. *Progress in Aerospace Sciences* 40: 321-343.
3. Zhoujie Lyu and Joaquim R. R. A. Martins (2014) Aerodynamic Shape Optimization Studies of a Blended-Wing-Body Aircraft. *Journal of Aircraft* 51: 1604-1617.
4. Li P, Zhang B, Chen Y, Yuan C, Lin Y (2012) Aerodynamic Design Methodology for Blended Wing Body Transport. *Chinese Journal of Aeronautics* 25: 508-516.
5. Schmollgruber P, Bartoli, J. Bedouet S, Defoort, Y. Gourinat (2017) Use of a Certification Constraints Module for Aircraft Design Activities. *American Institute of Aeronautics and Astronautics (AIAA)*
6. SU2 2018SU2. <https://su2code.github.io/>, June 24, 2018.
7. Garcia Cepeda 2018M. Garcia Cepeda. Design of Blended Wing Body: aerodynamic models. Master thesis, ISAE-SUPAERO, 2018.
8. ANSYS 2018 ANSYS. <https://www.ansys.com/>, June 24, 2018.
9. J.H. Ferziger (2002) *Computational Methods for Fluid Dynamics*. Springer, 2002.
10. OpenVSP 2018OpenVSP. July 30, 2018.
11. WP Dupont 2007 C. Colongo et W.P. Dupont. Preliminary Design of Commercial Transport Aircraft. AIRBUS, ISAE-SUPAERO, 2007
12. Kuethe 1997A.M. Kuethe et C.Y. Chow. *Foundations of Aerodynamics: Base of Aerodynamics Design*. John Wiley and Sons, New York, 1997.
13. Anderson JD. *Introduction to Flight*. McGraw-Hill, New York, 2011.
14. Cole JD, Cook Lp (1991)*Transonic Aerodynamics*, Volume 30. North Holland, 1991.
15. Nixon D (1982) *Transonic Aerodynamics*. American Institute of Aeronautics and Astronautics (AIAA).
16. Andan AD, Asrar W, Omar AA (2012) Investigation of Aerodynamic Parameters of a

- Hybrid Airship. Journal of Aircraft, vol. 49, no. 2.
17. Chapman CJ (2000) High Speed Flow. Cambridge University Press.
  18. Henne P (1990) Applied Computational Aerodynamics. American Institute of Aeronautics and Astronautics (AIAA).
  19. Kuchemann D (1978) The Aerodynamic Design of Aircraft. Pergamon Press.
  20. ONERA (2018) Office national d'études et de recherches aérospatiales. July 30, 2018
  21. Twaithes B (1960) Incompressible Aerodynamics. Dover, 1987.

**Copyright: ©2018 Luca Cerquetani<sup>1\*</sup>. This is an open-access article distributed under the terms of the Creative Commons Attribution License, which permit unrestricted use, distribution, and reproduction in any medium, provided the original author and source are credited.**